On Automatic Resonant Frequency Tracking in *LLC* Series Resonant Converter Based on Zero-Current Duration Time of Secondary Diode

Hong Li and Zhiyuan Jiang

***Abstract*—In order to achieve higher efficiency for the unregulated *LLC* series resonant converter, the switching frequency must be equal to the resonant frequency. However, since the converter works in open-loop condition, the switching frequency usually deviates from the resonant frequency in real converter. This paper proposed a new control method to track the resonant frequency of the unregulated *LLC* series resonant converter. Theoretically, the time of zero diode current in secondary is zero when the working frequency is equal or greater than the resonance frequency, and it is changed as the frequency varies when the working frequency is less than the resonance frequency. The proposed control algorithm is based on the time measurement of zero diode current to realize the resonance frequency tracking. A closed-loop digital controller is designed to realize the proposed tracking approach. The simulation and experiments are conducted to verify the proposed tracking approach. The simulation and experimental results show that (1) the switching frequency can be well controlled to track the resonant frequency, and (2) the tracking accuracy can be at least 96%.**

***Index Terms*—*LLC* series resonant converter, resonant frequency tracking, zero-current duration time.**

I. Introduction

IT is well known that the ultimate design goal of a power converter is to increase its power density, and the main approach to doing that is to increase switch frequencies. However, the increase of the frequency is constrained by switch losses. One way to deal with this difficulty is the soft-switch technology, in which the *LLC* converter has received much attention, due to its desired features: 1) the primary-side switch can be turned ON in zero voltage, 2) the switching-off losses can be absorbed by capacitors, and 3) the switch of the secondary rectifier diode has a zero current. Thus, the high efficiency and power density can be accomplished [1]–[6]. In conventional resonant converters, the switching frequency is used as a control variable to modulate the output voltage [7], [8] or to improve system's efficiency [9], [10]. In contrast, the unregulated *LLC* resonant converter, such as *LLC* dc–dc transformers, the desired working condition is realized by making the switching frequency equal to the resonant frequency. However, since the converter works in an open-loop condition, and the parameters of inductors and capacitors in the resonant tank are time-varying, the switching frequency usually deviates from the prescribed resonant frequency in most practical situations. Thus, in order to make an *LLC* converter operate at the resonant frequency, a resonant frequency tracking method is needed.

It is worthwhile to mention that the phase lock-loop is widely used in the frequency tracking in series resonant converter (SRC), parallel resonant converter, and *LLC* converter [11], [13], but it cannot be directly applied to isolated *LLC* SRC, because the tank input currents have asynchronous phases caused by the transformer magnetizing current. The study in [14] and [15] realize the frequency tracking by minimizing the pulse-width differences between primary-side main switches and secondary-side synchronous rectification driving signals. However, this method exploits the switching behavior by using an antiparallel diode MOSFET pair, which is not applicable for the diode bridge rectifier in the secondary. The study in [16] develops a resonant frequency tracking approach by using the minimum of total harmonic in the resonant current, but this method needs to calculate the total harmonic distortion of the resonant current online. The study in [1] proposes an automatic resonant frequency tracking scheme for a parallel *LLC* converter, where the drift in resonant frequency is detected by observing the phase relationship of an electrical variable pair, and it can be used in series *LLC* converter.

Based on the fact that the current flows in one direction at the resonant frequency, Li *et al.* [17] designed a resonant frequency tracking strategy in SRC. It is noted that this strategy is not workable, when the dc bus current is always bidirectional flowing. Since the DCdc bus current of the *LLC* is always bidirectional flowing in its working frequency domain, the proposed strategy in [17] cannot be applied for the *LLC* converter.

In this paper, we will propose a new *LLC* resonant frequency tracking approach by using the zero-current duration time of a secondary rectifier diode. This approach is only dependent on the zero-current duration time, and is independent *LLC* parameters. In addition, this approach is also very easy to be implemented in practice.

II. Signal Characteristics of Secondary Diode Current in *LLC* Converter

The circuit shown in Fig. 1 is equivalent to an *LLC* converter, where $R_{\rm ac}$ is the equivalent load, n is the transformer

Manuscript received August 31, 2014; revised May 23, 2015; accepted July 20, 2015. Date of publication July 29, 2015; date of current version January 28, 2016. Recommended for publication by Associate Editor F. Wang.

H. Li is with the School of Marine Science and Technology, Northwestern Polytechnical University, Xian 710072, China (e-mail: lihongja@nwpu.edu.cn).

Z. Jiang is with the School of Marine Science and Technology, Northwestern Polytechnical University, Xian 710072, China, and also with the Technology Center, FAW Group Corp., Changchun 130011, China (e-mail: jiangzhiyuan@rdc.faw.com.cn).

Digital Object Identifier 10.1109/TPEL.2015.2462086

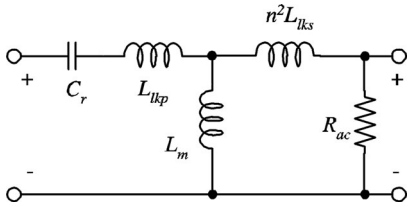

Fig. 1. Equivalent ac circuit of *LLC* converter.

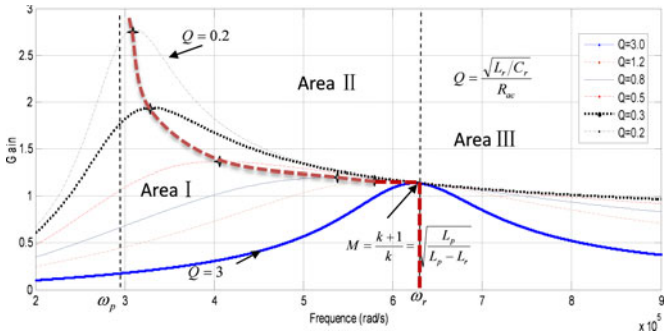

Fig. 2. Gain curves of *LLC*.

turning ratio, L_m is the magnetizing inductance of the transformer, and $L_{\rm lkp}$ and $L_{\rm lks}$ are the primary and secondary leakage inductance ($L_{\rm lkp} = n^2 L_{\rm lks}$), respectively. Let denote $k = L_m/L_{\rm lkp}, Q = \sqrt{L_r/C_r}/R_{\rm ac}, \omega_r = 1/\sqrt{L_r C_r}$ (i.e., resonant frequency), $\omega_p = 1/\sqrt{L_p C_r}$, then, $L_p = (k+1)L_{\rm lkp}$ and $L_r = L_{\rm lkp}(1 + k/(k+1))$. The equivalent impedance of the *LLC* is as follows:

$$z(j\omega) = \frac{\omega^2 L_m^2 R_{\rm ac}}{\omega^2(L_m + L_{\rm lkp})^2 + R_{\rm ac}^2} + j\left(\frac{\omega^2 L_{\rm lkp} C_r - 1}{\omega C_r} + \frac{\omega L_m \cdot [\omega^2 L_{\rm lkp}(L_m + L_{\rm lkp}) + R_{\rm ac}^2]}{\omega^2(L_m + L_{\rm lkp})^2 + R_{\rm ac}^2}\right). \quad (1)$$

The impedance angle is determined as

$$\alpha = {\rm arctg}\frac{\omega^4 L_{\rm lkp}^2(2k+1) + \omega^2 R_{\rm ac}^2(1 - Q^2\frac{(k+1)^2}{2k+1}) - R_{\rm ac}^2\omega_p^2}{\omega^3 L_m^2 L_p C_r R_{\rm ac}}. \quad (2)$$

The *LLC* gain is as follows:

$$M = \left|\frac{\left(\frac{\omega^2}{\omega_p^2}\right)\sqrt{\frac{L_p - L_r}{L_p}}}{j\left(\frac{\omega}{\omega_r}\right)\cdot\left(1 - \frac{\omega^2}{\omega_r^2}\right)\cdot Q\frac{L_p}{L_r} + \left(1 - \frac{\omega^2}{\omega_p^2}\right)}\right|. \quad (3)$$

The relations between different gains of Q and frequencies are shown in Fig. 2.

When $\alpha = 0$, and the equivalent impedance is pure resistive load, i.e.,

$$\omega^4(2k+1)L_{\rm lkp}^2 - R_{\rm ac}^2\omega_p^2 + \omega^2 R_{\rm ac}^2\left[1 - Q^2\frac{(k+1)^2}{2k+1}\right] = 0. \quad (4)$$

The solution to (4) is the working frequency of the pure resistive load, i.e., the peak gain frequency ω_{pp}. When the circuit parameters are fixed in (4), the peak gain frequency

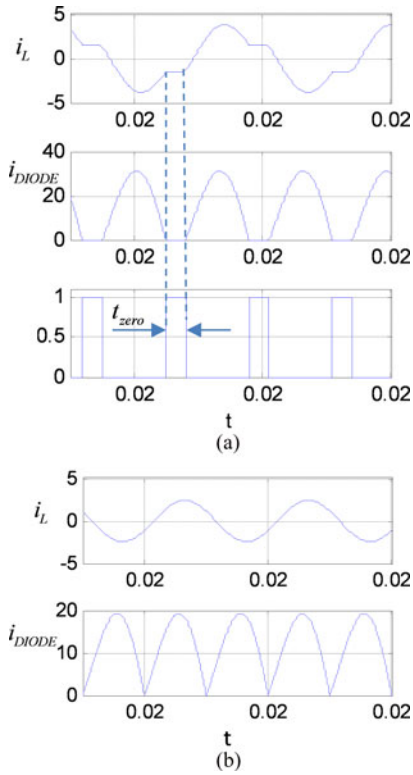

Fig. 3. $t_{\rm zero}$ and ω. (a) $\omega_{pp} < \omega < \omega_r$. (b) $\omega \geq \omega_r$.

change as Q (i.e., the load) varies. In particularly, when $Q = 0$ (i.e., $R_{\rm ac} = \infty$), $\omega^4(2k+1)L_{\rm lkp}^2/R_{\rm ac}^2 - \omega_p^2 + \omega^2 = 0$, leading to $\omega_{pp} = \omega_p$; when $Q = \infty$, (i.e., $R_{\rm ac} = 0$), $\omega^2(2k+1)L_{\rm lkp}^2 - \frac{L_r}{C_r}\frac{(k+1)^2}{2k+1} = 0$, leading to $\omega_{pp} = \omega_r$. Therefore, the peak gain frequency will change from ω_p to ω_r, as the load changes from an open-circuit case to a short-circuit case in the *LLC* SRC. The peak gain point is labeled as "$*$" in Fig. 2.

When $\omega_{pp} < \omega < \omega_r$, the equivalent load of *LLC* is inductive, the main switches turn ON in zero-voltage condition, and the secondary rectifier diodes turn ON and OFF in zero-current condition. The related waveforms are demonstrated in Fig. 3(a), where i_L is the resonant current, $i_{\rm DIODE}$ is the current of the secondary rectifier diodes, and $t_{\rm zero}$ is the duration time when $i_{\rm DIODE} = 0$. When $\omega \geq \omega_r$, the related waveforms are demonstrated in Fig. 3(b).

From Fig. 3, it can be seen that, (1) when $\omega_{pp} < \omega < \omega_r$, $t_{\rm zero}$ change as frequency varies, and (2) when $\omega \geq \omega_r$, $t_{\rm zero}$ is always zero. When the load steps from 2 to 1Ω and the switch frequency is equal to ω_r, the step transient response is shown in Fig. 4, from which it can be observed that the load change does not affect $t_{\rm zero}$.The relationship between ω ($T = 2\pi/\omega$) and $t_{\rm zero}/T$ is shown in Fig. 5, from which it can be seen that when $\omega \geq \omega_r$, $t_{\rm zero} = 0$ (that is, $t_{\rm zero}/T = 0$); when $\omega_{pp} < \omega < \omega_r$, $t_{\rm zero}/T$ change as the frequency varies. Thus, $t_{\rm zero}/T$ or $(1 - t_{\rm zero}/T)$ can be used as a basis to determine, whether the *LLC* converter works at resonant frequency or not.

In the application for the H Bridge, the dead time always exists, so we need to analyze the effect of dead time on $t_{\rm zero}$. Because the *LLC* equivalent load is inductive when $\omega \geq \omega_{pp}$, the

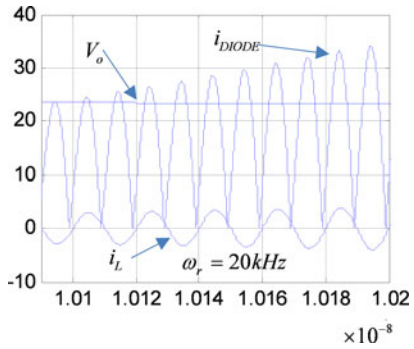

Fig. 4. Load step-up transient ($\omega = \omega_r, t_{\rm zero} = 0$).

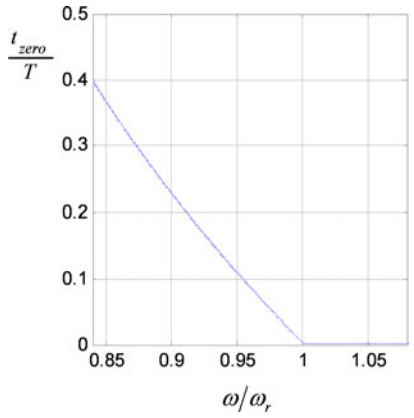

Fig. 5. Relation between ω and $t_{\rm zero}/T$ ($\omega > \omega_{pp}$).

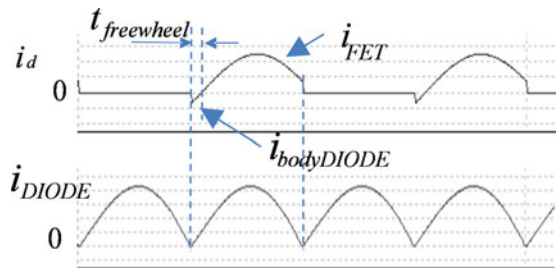

Fig. 6. Example to show the maximum $t_{\rm freewheel}$.

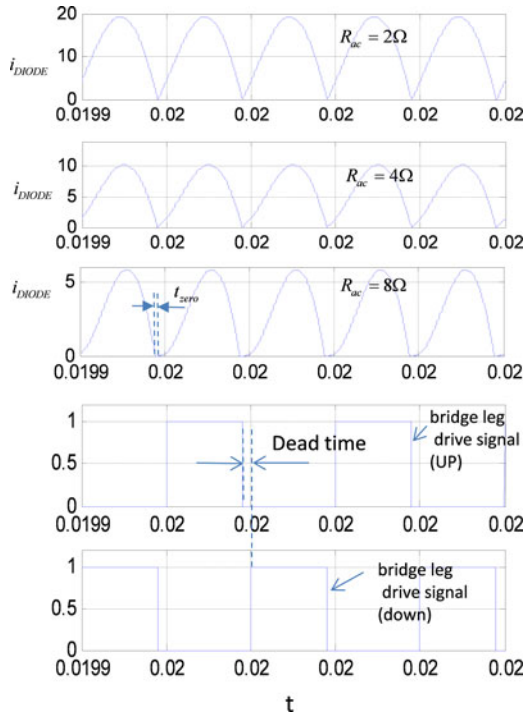

Fig. 7. Effect of load decreases to $t_{\rm zero}$.

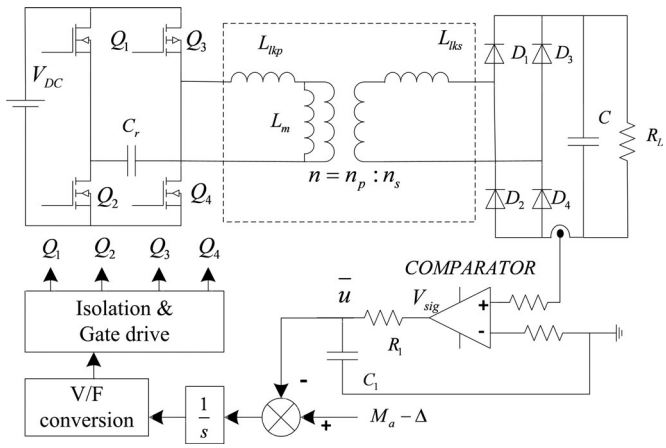

Fig. 8. Proposed resonant frequency tracking approach.

current flows through the body diode of main switches during the dead time. Based on (2), if the parameters of the *LLC* converter are kept unchanged, then the impedance angle α only depends on $R_{\rm ac}$ and ω. Let the time corresponding to α be the maximum freewheeling time and can be written as $t_{\rm freewheel} = \alpha/\omega$. Due to the fact that the freewheeling current depends on load current, this method may be not suitable for light loads. To demonstrate this point, we provide Figs. 6 and 7 in the following as examples to show the detailed reason. In Fig. 6, i_d is the current of any MOSFET in H Bridge, $i_{\rm bodyDIODE}$ and $i_{\rm FET}$ are the currents flowing through the body diode and FET in MOSFET, respectively. When the load is light, the $i_{\rm bodyDIODE}$ may be equal to the excitation current of the transformer, and the output current of the rectifier diode approaches to zero which affects the $t_{\rm zero}$.

Fig. 7 shows the influence of load on $t_{\rm zero}$, when the dead time is fixed and $\omega = \omega_r$. It can be seen that the $t_{\rm zero}$ may be larger than zero as the load current decreases significantly, and this method might not be suitable. It is worth noting that, according to the simulation and experiments, this method is still workable when the load decreases to 30% of the rated load.

III. Proposed Resonant Frequency Tracking Approach

The proposed resonant frequency tracking approach is shown in Fig. 8. The challenge of using $1 - t_{\rm zero}/T$ to track the resonant frequency comes from the measurement of the $t_{\rm zero}$. Since $t_{\rm zero}$ is almost zero when $\omega \geq \omega_r$, it is rather difficult to directly measure an accurate $t_{\rm zero}$. Here, we adopt an indirect method

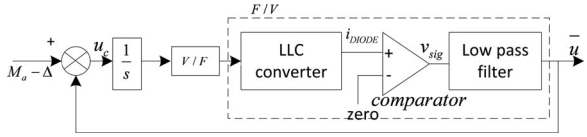

Fig. 9. Control black diagram of resonant frequency tracking.

to measure it, and the procedure is described as follows: First, $i_{\rm DIODE}$ is measured by the Hall current sensor, then $i_{\rm DIODE}$ is converted to a pulse signal $v_{\rm sig}$ by using the crossing-zero comparator. Finally, the average value of $v_{\rm sig}$(i.e., $\overline{u}$) is obtained by using the *RC* low-pass filter. Note that this method proposes to measure the average value instead of directly measuring $t_{\rm zero}$, which greatly simplifies the measurement processes; although the using of the *RC* low-pass filter will cause the delay issue on frequency tracking.

If the magnitude of $v_{\rm sig}$ is M_a, the average value of $v_{\rm sig}$ is

$$\overline{u} = M_a(1 - t_{\rm zero}/T) = M_a(1 - t_{\rm zero}\omega/2\pi). \tag{5}$$

From (5), we can see that $\overline{u}$ only depends on the magnitude M_a and $t_{\rm zero}/T$. If $\omega \geq \omega_r$, $\overline{u} = M_a$; if $\omega_{pp} < \omega < \omega_r$, $\overline{u}$ is a function of ω. Note that $\overline{u}$ is always equal to M_a in the range of $\omega \geq \omega_r$, it is difficult to determine the exact value of ω_r. When $\omega_{pp} < \omega < \omega_r$, the value of $\overline{u}$ can be uniquely determined by ω, implying that $\overline{u}$ reflects the variations of working frequency in an *LLC* converter.

Assume that $\Delta \ll M_a$. Based on the aforementioned idea, we use $M_a - \Delta$ as the reference signal, and $\overline{u}$ as the feedback of the working frequency of the *LLC* converter in the control closed-loop, shown in Fig. 9, where the resonant frequency ω_r can be obtained approximately, and is called the quasi-resonant frequency ω_{qr}. Obviously, ω_{qr} is always less than ω_r. In this design, the less Δ is the better ω_{qr} approaches to ω_r. However, Δ cannot be too small, and must be greater than the sampling resolution of A/D conversion.

In Fig. 9, *V/F* represents the conversion from voltage to frequency; the dashed box is equivalent to the conversion from the frequency to voltage. Denoting the conversion ratio in *V/F* by k_1, the output of *V/F* conversion can be written as

$$\omega_n = \omega_{n-1} + \frac{k_1}{s}u_c = \omega_{n-1} + \frac{k_1}{s}(M_a - \Delta - \overline{u}). \tag{6}$$

The program flowchart of the control closed-loop described in Fig. 9 is shown in Fig. 10, where ω_0 is the initial working frequency, and the final value of ω_n is the desired ω_{qr}.

There are two choices to determine the initial working frequency ω_0, i.e., $\omega_0 < \omega_r$ and $\omega_0 > \omega_r$. In Section II, we know that $|\omega_r - \omega_{pp}|$ decreases as the load increases. If we take the first choice, ω_0 will vary as the load changes, otherwise the *LLC* SRC may be operated at the frequency $\omega_0 < \omega_{pp}$, which is not desirable. If the second choice is taken, we can avoid the effects caused by load change; therefore, the second choice is preferred.

The *LLC* converter can be equivalent to an amplifier with a pure time delay as follows:

$$\frac{i_L(s)}{u_{ct}(s)}\Big|_{\omega=\omega_n} = Ke^{-T_1 s} \approx \frac{K}{T_1 s + 1} \tag{7}$$

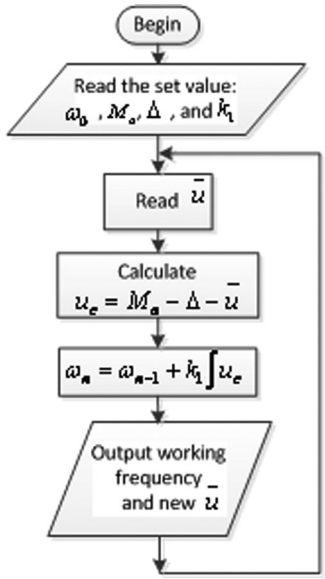

Fig. 10. Program flowcharts.

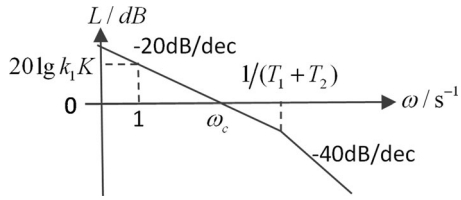

Fig. 11. Open loop logarithm amplitude frequencies curve.

where the gain of *LLC* converter is K, u_{ct} is the *V/F* output, T_1 is delay time of the *LLC* converter, and in general, T_1 is equal to the switching cycle. The low-pass filter can be written as

$$\frac{\overline{u}(s)}{i_L(s)} = \frac{1}{T_2 s + 1} = \frac{1}{R_1 C_1 s + 1}. \tag{8}$$

In general, the $T_2 \gg T_1$ (i.e., $R_1C_1 \gg T_1$). As a result, the *F/V* conversion can be approximately simplified as

$$\frac{\overline{u}(s)}{u_{ct}(s)} = \frac{K}{T_1 s + 1} \cdot \frac{1}{T_2 s + 1} \approx \frac{K}{(T_1 + T_2)s + 1}. \tag{9}$$

By using an integral regulator, the transfer function in (9) can tranformed into the typical type I system or a typical two order system. The forward path transfer functionn can be expressed as

$$G(s) = \frac{k_1 K}{s[(T_1 + T_2)\, s + 1]}. \tag{10}$$

The open-loop logarithm amplitude frequency response is shown in Fig. 11.

In order to increase the stability of the system, the logarithmic amplitude–frequency curve should be –20 dB/dec slope across the 0 dB line. As a result, $\omega_c < 1/(T_1 + T_2)$. From Fig. 11, we can obtain $L(\omega)\,|_{\omega=1} = 20\lg k_1 K = 20\lg \omega_c$, leading to $k_1 K = \omega_c$.Therefore, $k_1 K(T_1 + T_2) < 1$. The closed-loop responses of the system with three different k_1 are shown in Fig. 12.

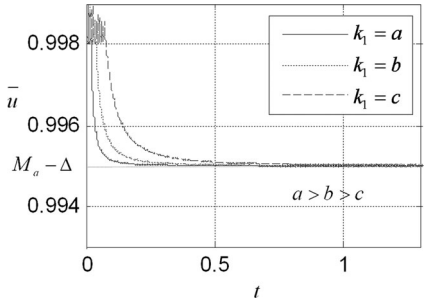

Fig. 12. Closed-loop responses with different k_1.

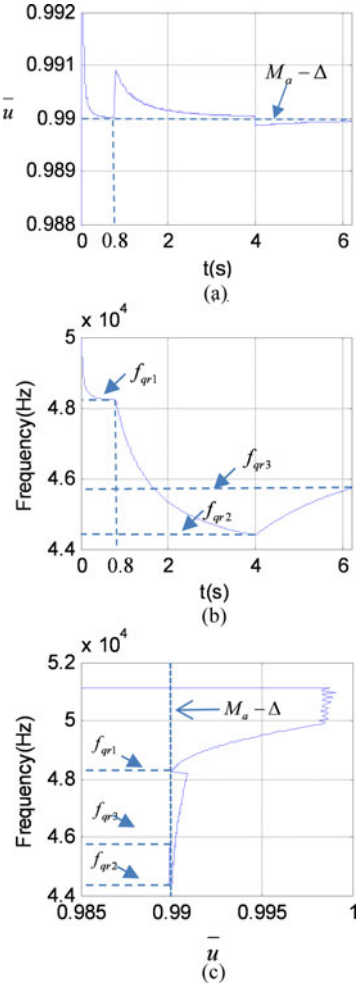

Fig. 13. Relation between the working frequency and $\overline{u}$.

The simulation results of the closed-loop resonant frequency tracking are shown in Fig. 13. At the beginning $\omega_0 > \omega_r$, the switching frequency will gradually decrease to f_{qr1}, and at the same time $\overline{u}$ also gradually approaches to $M_a - \Delta$ (see Fig. 13, $M_a - \Delta = 0.99$). At time $t = 0.8\,\mathrm{s}$, the resonant capacity C_r increases, implying that ω_r decreases. As a result, $\overline{u}$ is larger than $M_a - \Delta$, leading to $u_c < 0$. As the time increases, the working frequency will decrease and the $\overline{u}$ will also be gradually reduced to $\overline{u} = M_a - \Delta$. That is, the working frequency of the *LLC* converter will gradually approach to the new quasi-resonance frequency f_{qr2}. At time $t = 4\,\mathrm{s}$, the resonant capacity C_r decreases that means ω_r also increases. As a consequence, $\overline{u}$ is less than $M_a - \Delta$, resulting in $u_c > 0$. That is, the working frequency will increase and $\overline{u}$ will also gradually be reduced to $\overline{u} = M_a - \Delta$. In this case, the working frequency will gradually approach to another new quasi-resonance frequency f_{qr3}.

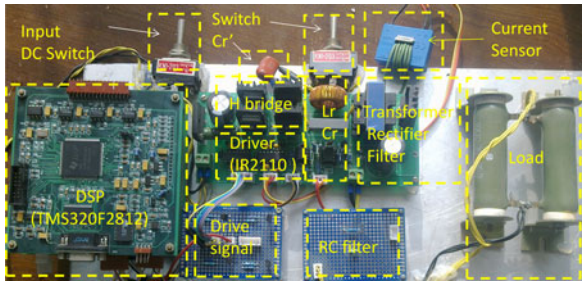

Fig. 14. Experiment bed.

IV. Experiments and Verification

The *LLC* SRC experiment bed is shown in Fig. 14. Here, the DSP (TMS320F2812) is used as the controller to provide the working frequency of *LLC* converter and generate the drive signals of the H bridge; the H bridge is built by MOSFET, and the current sensor is Hall current sensor (the power loss is about 2 W). To meet the input voltage range (0–3 V) of A/D in DSP, the maximum value of $\overline{u}$ is designed to be 2.1 V, that is, M_a is equal to 2.1 V; the selection of the minimum value $\Delta_{\min}$ should be more than the resolution of A/D converter, theoretically, but in practice, $\Delta_{\min}$ is at least one order of magnitude larger than the resolution of A/D converter. For example, the A/D converter in TMS320F2812 is 10 bit and the resolution is 3/1024, then $\Delta_{\min} = 0.029$.

The parameter variation of the resonant tank is simulated by a circuit in which two capacitors (i.e., Cr and C_{r}') are connected in parallel, and a switch is connected in series with C_{r}'. By turning the switch ON and OFF the parameter variations can be mimicked. The parameters are designed as follows: $C_r' = 7\,\mathrm{nF}$(the standard value is 6.8 nF), $C_r = 0.038\,\mu\mathrm{F}$(the standard value is 0.033 μF), $L_r = 762\,\mu\mathrm{H}$, the input voltage is 50 V, the transformer turns ratio n is $2:1$, and the maximum output power is 180 W. When switching on (off) C_r', the resonant frequency of the *LLC* converter is $f_r \approx 27179\,\mathrm{Hz}$ ($f_r \approx 29576\,\mathrm{Hz}$).

As mentioned above, the proposed method is based on t_{zero}. Therefore, in the experiment, we first need to verify the effectiveness of the measurement method of t_{zero} in the open loop. The procedure is as follows: Open the feedback loop of $\overline{u}$, set the working frequency of the *LLC* converter (which is generated by DSP), and gradually decrease starting from ω_0. In the procedure, the current i_{DIODE} and t_{zero} at different working frequencies are shown in Fig. 15.

Note that in Fig. 15, the i_{DIODE} during t_{zero} has noises in the experiments. The noises make the v_{sig} deviate from the ideal shape, so the V_{avg} (i.e., $\overline{u}$) obtained by using a RC low-pass

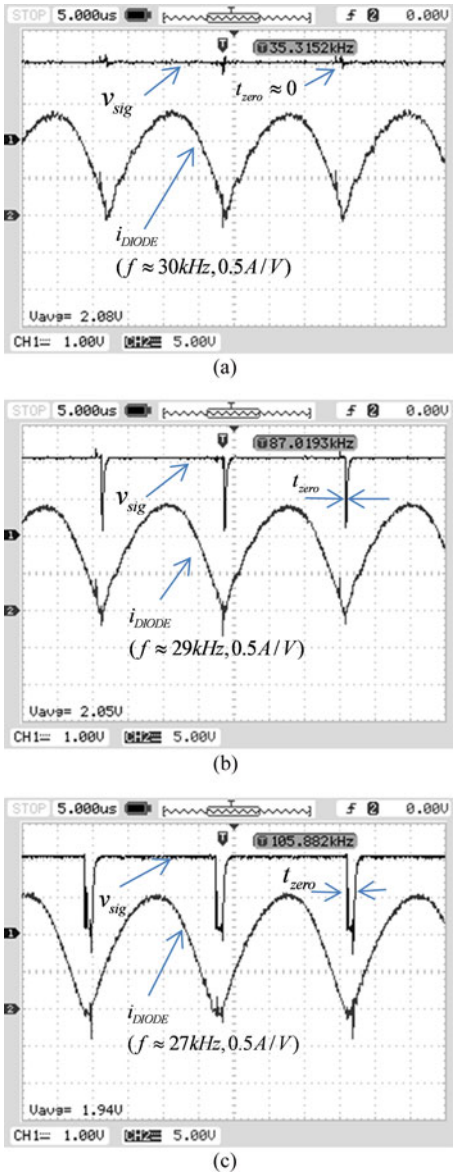

Fig. 15. Secondary diode current and the pulse signal v_{sig}.

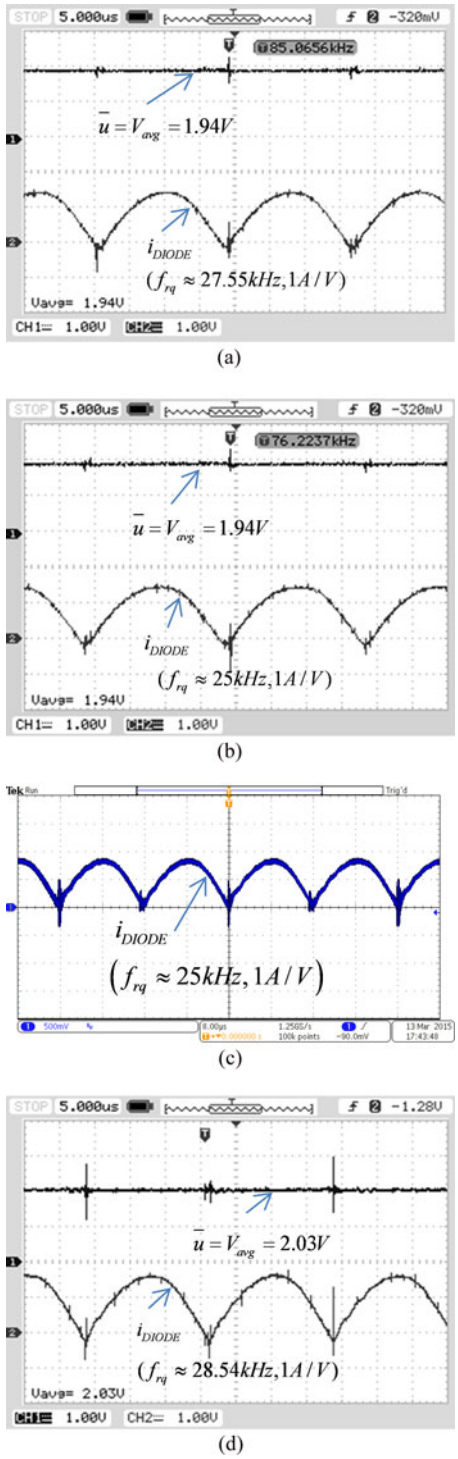

Fig. 16. Frequency tracking for different resonant capacitances.

filter will change accordingly. Also, despite the presence of noise when $\omega \approx \omega_r$, the t_{zero} is almost zero. This means that the $\overline{u}$ is insensitive to noises at the working frequency $\omega \approx \omega_r$. Since the proposed method is used to approximate tracking resonant frequency $\omega \approx \omega_r$, where $\overline{u}$ is not sensitive to noises, this approach is still valid in practical applications.

Second, we need to verify the closed-loop performance. Close the feedback loop of $\overline{u}$, and then three cases are considered:

1) Switch off the the capacitor C_r' (i.e.,$C_r = 0.038\,\mathrm{uF}$), and set $\Delta = 0.16$ (that means $M_a - \Delta = 1.94$) and $k_1 = 10$. The responses of $\overline{u}$ and i_{DIODE} are shown in Fig. 16(a), where the quasi-resonance frequency is $f_{qr} \approx 27.55\,\mathrm{kHz}$ and $\overline{u}$ is equal to the reference value ($\overline{u} = M_a - \Delta = 1.94\,\mathrm{V}$). From Fig. 16(a), it can be seen that the closed-loop system is stable, and the relative error of resonance frequency tracking is $(f_r - f_{qr})/f_r \approx 9\%$.

2) Switch ON the capacitor C_r'(i.e., $C_r + C_r' = 0.045\,\mathrm{uF}$, $f_r \approx 27179\,\mathrm{Hz}$), and the other parameters are the same as 1) the tracking frequency is about 25 000 Hz, as shown in Fig. 16(b). The relative error of the resonance frequency tracking is $(f_r - f_{qr})/f_r \approx 8\%$ and $\overline{u}$ is always equal to $M_a - \Delta = 1.94\,\mathrm{V}$. When the load decreases to the half of its original, the tracking frequency stays the same and the current decreases nearly to its half, as shown in Fig. 16(c).

3) Reduce Δ to 0.06 V (i.e.,$M_a - \Delta = 2.03\,\mathrm{V}$) and keep $C_r = 0.038\,\mathrm{uF}$. After the experiment, the tracking frequency is about 28.54 kHz, which is record in Fig. 16(d). The relative error of resonance frequency tracking is $(f_r - f_{qr})/f_r \approx 3.8\%$, and $\overline{u}$ is equal to $M_a - \Delta = 2.03\,\mathrm{V}$. This verifies that reducing Δ can decrease the tracking error, making the quasi-resonant frequency approach to the resonant frequency. The experiment shows that the proposed method in the experiment bed can get at least 96% accuracy.

As mentioned above, the design instructions for practical controller design can be summarized as follows:

Step 1): Calculate the theoretical resonant frequency of the design *LLC* converter. Step 2): Determine the initial frequency ω_0 and let $\omega_0 = 1.2\,\omega_r$. Step 3): Determine $\Delta_{\min}$. Let $\Delta_{\min} = 10x_{\mathrm{res}}$, where x_{res} is the resolution of the A/D. Step 4): Determine T_1, T_2, K, and k_1. Based on ω_r, obtain T_1 and let $T_2 = 10T_1$; based on $k_1K(T_1 + T_2) < 1$, determine k_1 and let $k_1 = 1/[2K(T_1 + T_2)]$.

V. Conclusion

This paper has developed a new resonant frequency tracking approach for a *LLC* SRC. In this approach, the zero-current duration time of the secondary diode has been used as a basis to determine whether the *LLC* SRC reaches resonance or not. In particular, the detailed ideas under this approach and in-depth analysis on how to reach automatic tracking are also provided. The proposed approach is only affected by the time when the current is equal to zero, and is independent of *LLC* parameters. Therefore, it can be applied to the *LLC* converters of any power level. Another notable feature of the proposed approach is easy to be implemented in practice. The effectiveness of the proposed approach is verified by simulation and experimental results. Note that the proposed method might not be suitable for very slight load as we explained. So, how to determine the theoretical load range when the method is valid is our future study topic.

References

[1] U. Kundu, P. Chakraborty, and S. Sensarma, "Automatic resonant frequency tracking in parallel *LLC* boost DC–DC converter ," *IEEE Trans. Power Electron.*, vol. 30, no. 7, pp. 3925–3933, Jul. 2015.

[2] Z. Guo, D. Sha, and X. Liao, "Hybrid phase-shift-controlled three-level and LLC DC–DC converter with active connection at the secondary side ," *IEEE Trans. Power Electron.*, vol. 30, no. 6, pp. 2985–2996, Jun. 2015.

[3] B. Lu, W. Liu, Y. Liang, F. C. Lee, and J. D. Van Wyk, "Optimal design methodology for LLC resonant converter," in *Proc. IEEE Appl. Power Electron. Conf.*, 2006, pp. 533–538.

[4] T. Liu, Z. Zhou, A. Xiong, J. Zeng, and J. Ying, "A novel precise design method for LLC series resonant converter," in *Proc. IEEE Int. Telecommun. Energy Conf.*, 2006, pp. 1–6.

[5] F. Yang, C. Lee, A. J. Zhang, and G. Huang, "LLC resonant converter for front end DC/DC conversion," in *Proc. IEEE Appl. Power Electron. Conf.*, 2002, pp. 1108–1112.

[6] W. Feng, F. C. Lee, P. Mattavelli, C. Prasantanakorn, and D. Huang, "LLC resonant converter burst mode control with constant burst time and optimal, switching pattern," in *Proc. IEEE Appl. Power Electron. Conf.*, 2011, pp. 6–12.

[7] J. Y Lee, Y. S. Jeong, H. J. Chae, K. M. Yoo, J. J. Chang, and J. H. Chang, "Two-stage insulated bidirectional DC/DC power converter using a constant duty ratio LLC resonant converter," U.S. Patent 20 111 009 071 7A1, Apr. 21, 2011.

[8] R. L. Steigerwald, "A comparison of half-bridge resonant converter topologies," *IEEE Trans. Power Electron.*, vol. 3, no. 2, pp. 174–182, Apr. 1988.

[9] F. C. Lee, S. Wang, P Kong, C. Wang, and D. Fu, "Power architecture design with improved system efficiency, EMI and power density," in *Proc. IEEE Power Electron. Spec. Conf.*, 2008, pp. 4131–4137.

[10] J.-B. Lee, J.-K. Kim, J.-H. Kim, J.-I. Baek, and G.-W. Moon, "A high-efficiency PFM half-bridge converter utilizing a half-bridge *LLC* converter under light load conditions," *IEEE Trans. Power Electron.*, vol. 30, no. 9, pp. 4931–4942, Sep. 2015.

[11] T. J. Liang and J. J. Ribarich, "A new procedure for high-frequency electronic ballast design," *IEEE Trans. Ind. Appl.*, vol. 37, no. 1, pp 262–267, Jan./Feb. 2001.

[12] H. S. Heng, Y. Pei, X. Yang, F. Wang, and C. W. Tipton, "Frequency tracking control for cap-charging parallel resonant converter with phase-locked loop," in *Proc. IEEE Appl. Power Electron. Conf. Expo.*, 2007, pp. 1287–1292.

[13] Y. Yin, M. Shirazi, and R. Zone, "Electronic ballast control IC with digital phase control and lamp current regulation," *IEEE Trans. Power Electron.*, vol. 23, no. 1, pp. 11–18, Jan. 2008.

[14] W. Feng, P. Mattavelli, and F. C. Lee, "Pulse width locked loop (PWLL) for automatic resonant frequency tracking in LLC DC-DC transformer (LLC-DCX)," *IEEE Trans. Power Electron.*, vol. 28, no. 4, pp. 1862–1869, Apr. 2013.

[15] W. Feng, P. Mattavelli, F. C. Lee, and D. Fu, "LLC converters with automatic resonant frequency tracking based on synchronous rectifier (SR) gate driving signals," in *Proc. IEEE Appl. Power Electron. Conf. Expo.*, 2011, pp. 1–5.

[16] S. Jiang, W. Zhang, B. Liu, and F. Wang, "Automatic resonant frequency tracking in unregulated LLC resonant converters based on total resonant current harmonic calculation," in *Proc. IEEE Energy Convers. Congr. Expo.*, 2013, pp. 4193–4198.

[17] H. Li, Y. He, and C. Wang, "A new method of frequency tracking and output power control for full bridge series load resonant inverter," *Trans. China Electrotech. Soc.*, vol. 25, no. 7, pp. 93–99, Jul. 2010.

Hong Li was born in Yuanqu, Shaanxi, China, in 1962. He received the B.S., M.S., and Ph.D. degrees in control theory and control engineering from Northwestern Polytechnical University (NPU), Xi'an, China, in 1985, 1997, and 2007, respectively.

From 1985 to 1989, he was an Assistant Professor with the Department of Mechanical Engineering, NPU, where he joined the School of Marine Science and Technology in 1990, and is currently an Associate Professor. From 2012 to 2013, he was a Visiting Scholar with the Department of Electrical Engineering, The University of Tennessee, Knoxville, USA. He is the Author of three books and more than 30 articles in major journals of China. His recent research interests include motor control and resonant power supply.

Zhiyuan Jiang was born in Changchun, Jilin, China, in 1988. He received the B.S. and M.S. degrees in control theory and control engineering from Northwestern Polytechnical University, Xi'an, China, in 2012 and 2015, respectively.

Since April 2015, he has been an Assistant Research with the Technology Center, FAW Group Corp., Changchun, China. His research interest includes switching mode power supply and motor control.